Control and verification of the safety-factor profile in tokamaks using Sum-of-Squares polynomials.

A. Gahlawat * **M. M. Peet** ** **E. Witrant** ***

* *Cybernetic Systems and Controls Lab.(CSCL), Department of Mechanical, Materials and Aerospace Engineering, Illinois Institute of Technology, Chicago, Il 60616 USA (e-mail: agahlawa@iit.edu).*
** *Department of Mechanical, Materials and Aerospace Engineering, Illinois Institute of Technology, Chicago, Il 60616 USA (e-mail: mpeet@iit.edu)*
*** *Automatic Control Department of GIPSA-lab, University Joseph Fourier, Grenoble, France, (e-mail: emmanuel.witrant@gipsa-lab.grenoble-inp.fr)*

Abstract: In this paper, we propose a method of using the sum-of-squares methodology to synthesize controllers for plasma stabilization in Tokamak reactors. We use a partial differential model of the poloidal magnetic flux gradient and attempt to stabilize a reference safety-factor profile. Our methods utilize full-state feedback control and are based on solving a dual version of the Lyapunov operator inequality. In addition, we implement the controller in-silico using experimental conditions inferred from the Tore Supra tokamak.

1. INTRODUCTION

Fossil fuel energy or cheap energy, as known in the common vernacular, until now has been responsible for quenching the ever increasing energy demands of the world. However, since fossil fuel reserves are limited, we would inevitably reach a maximum extraction rate of petroleum also known as *oil peak*. Once this *oil peak* is achieved there would be an energy shortfall. There is a general consensus that we will reach the *oil peak* sometime in the next five decades Campbell and Laherrère [1998]. To fill the resultant energy shortfall various sources of energy are being investigated. One of the sources being currently researched is nuclear fusion wherein two light nuclei are fused together to produce a heavier nucleus and energy. Energy production using nuclear fusion has various advantages such as being clean and the ability to provide energy for several thousands of years Pironti and Walker [2005]. Among the different possibilities to achieve sustained fusion reactions the tokamak magnetic configuration, which motivated the ITER project, appears as the most promising.

The development of control protocols for tokamak plasmas is highly challenging, due to the high order of the distributed dynamics associated with non-homogeneous transport phenomena, the multiple time-scales involved Moreau et al. [2008] and the instabilities associated with the magneto-hydro-dynamic phenomena Connor et al. [1998]. Additionally, several stabilization and regulation problems have to be solved using a limited number of actuators that have a relatively few degrees of freedom. Therefore to make thermonuclear fusion an economically viable source of energy, several extremely demanding control problems have to be solved.

An important physical quantity related to the control of non-homogeneous transport is the magnetic field line pitch profile, also known as the *safety factor profile* or the q-profile Wesson and Campbell [2004]. The q-profile is a common heuristic for setting operating conditions that avoid undesired MHD instabilities Moreau et al. [2008],Eriksson et al. [2002]. Additionally, recent studies have shown the importance of the q-profile in triggering internal transport barriers (ITB) Eriksson et al. [2002], Tala et al. [2001], Garbet et al. [2003], which significantly improve the energy confinement, or in generating saw teeth that allow to remove the fusion ashes from the central plasma.

The safety factor profile is defined as the ratio of toroidal versus poloidal magnetic flux gradients. Neglecting the diamagnetic effect and thanks to the cylindrical approximation, the safety factor profile is defined in terms of the poloidal flux $\psi(x,t)$ as Witrant et al. [2007]

$$q(x,t) \doteq \frac{\partial\phi/\partial x}{\partial\psi/\partial x} = \frac{-B_{\phi_0}a^2x}{\partial\psi/\partial x}, \qquad (1)$$

where x is the normalized radius, t is time, B_{ϕ_0} is the toroidal magnetic field at the plasma center, a is the radius of the last closed magnetic surface(LCMS) and ϕ is the magnetic flux of the toroidal field. Thus to control the q-profile we control the gradient of the flux of the poloidal magnetic field, or ψ_x. In this paper we outline a method for designing controllers for regulating the gradient of the flux of the poloidal field, $\psi_x(x,t)$, about a desired reference profile.

Most of the previous results on tokamak poloidal flux control relied on linear finite-dimensional control theory applied to a discretized transport model Blum [1988], Ariola and Pironti [2008], Firestone [2007]. We aim to design an infinite dimensional controller for the dynamics of $\psi_x(x,t)$ described by a PDE, thus excluding the need to discretize the system model into a system of ODEs. Synthesis of infinite-dimensional controllers for PDEs has been studied in the context of distributed parameter systems theory, with some interesting examples given in Curtain and Zwart [1995]. In this paper we use the sum-of-squares (SOS) framework and semidefinite programming (SDP) to find polynomial gains for a state feedback controller such that we can construct a Lyapunov function Lyapunov [1992] algorithmically for the controlled system.

Note that the method for constructing Lyapunov functions algorithmically for PDEs using SOS polynomials is formulated in Papachristodoulou and Peet [2007]. In addition to systems described by PDEs, similar approaches have been used to construct Lyapunov functions for other infinite dimensional systems such as systems described by delay differential equations Peet et al. [2007].

We implement our approach using SOSTOOLS Prajna et al. [2001], a freely available MATLAB toolbox used for running algorithms for optimization, using SDP, over the set of SOS polynomials.

The paper is arranged as follows. In section II background material is provided for the system model, SOS polynomials and Lyapunov stability theory for systems whose state space acts on infinite dimensional spaces. In Section III we formulate the problem to be solved. In Section IV we provide a discretization scheme to numerically solve the controlled PDE and finally in Section V results are provided for a controller synthesized using the method outlined in the paper.

2. PRELIMINARIES

2.1 Tore Supra poloidal magnetic flux model

Neglecting the diamagnetic effect and thanks to the cylindrical approximation of the plasma shape, the poloidal flux diffusion model presented in Blum [1988] was simplified and completed with peripheral physical variables definitions associated with Tore Supra automation in Witrant et al. [2007] to get

$$\frac{\partial \psi(x,t)}{\partial t} = \frac{\eta_{\parallel}(x,t)}{\mu_0 a^2}\frac{1}{x}\frac{\partial}{\partial x}\left(x\frac{\partial \psi(x,t)}{\partial x}\right) + \eta_{\parallel}(x,t) R_0 j_{ni}(x,t).$$

where μ_0 is the permeability of free space, $\eta_{\parallel}(x,t)$ the plasma resistivity and $j_{ni}(x,t)$ the non-inductive current density. $j_{ni}(x,t)$ can be written as the sum of external non-inductive current density and internally generated bootstrap current density, or

$$j_{ni}(x,t) = j_{eni}(x,t) + j_{bs}(x,t),$$

where, $j_{eni}(x,t)$ is the external non-inductive current density and $j_{bs}(\rho,t)$ is the bootstrap current density.

The dynamics of ψ_x, necessary to compute the q-profile as detailed in (1), is obtained by differentiating the above equation with respect to x as:

$$\frac{\partial \psi_x(x,t)}{\partial t} = \frac{1}{\mu_0 a^2}\frac{\partial}{\partial x}\left(\frac{\eta_{\parallel}(x,t)}{x}\frac{\partial}{\partial x}\left(x\psi_x(x,t)\right)\right) + \dots$$
$$+ R_0 \frac{\partial}{\partial x}\left(\eta_{\parallel}(x,t) j_{ni}(x,t)\right). \quad (2)$$

The boundary condition at the plasma center ($x = 0$) is

$$\psi_x(0,t) = 0. \quad (3)$$

On the LCMS ($x = 1$) the boundary condition is dictated by the external current carrying coils as

$$\psi_x(1,t) = -\frac{R_0 \mu_0 I_p(t)}{2\pi}, \quad (4)$$

where the current in the external coils is controlled as required for the desired plasma current $I_p(t)$.

2.2 Sum-of-Squares Polynomials

Sum-of-Squares is a powerful tool for optimization over the convex cone of positive polynomials. By definition, a polynomial $p(x)$ is *sum-of-squares* (SOS) if it can be expressed as

$$p(x) = \sum_{i=1}^{N} p_i(x)^2,$$

where $p_i(x)$, $i = 1, \cdots, N$ are polynomials. Since any squared polynomial is non-negative, a SOS polynomial $p(x)$ will be non-negative. Although the question of polynomial positivity is NP-hard Blum [1998], the question of whether a polynomial is SOS is tractable due to the following result.

Theorem 1. A polynomial $p(x)$, $x \in \mathbb{R}^n$ of degree $2d$ is sum-of-squares iff there exists a positive semidefinite matrix $Q \succeq 0$ such that

$$p(x) = Z(x)^T Q Z(x), \quad (5)$$

where $Z(x)$ is a vector of all possible monomials of degree d or less.

This theorem implies that we can test whether a polynomial is sum-of-squares using semidefinite programming. Since it is generally accepted that SDPs can be solved in polynomial time using interior point methods Nesterov and Nemirovsky [1994], the problem of checking whether a polynomial can be expressed as a sum of squared polynomials is tractable.

In this paper we will use SOS programming to ensure positivity/negativity of integrals with polynomial integrands. For example, suppose we have the following integral with a polynomial integrand

$$V(t) = \int_{\Omega} p(x,t)dx,$$

where Ω is a subset of a complete metric space, $x \in \mathbb{R}$ and $t \in \mathbb{R}_+$. A sufficient condition for $V(t) \geq 0$ is that $p(x,t)$ be a SOS polynomial.

2.3 Lyapunov stability theory

In this section we will provide some background on stability. In addition, the well known *Lyapunov stability* theorem is also provided which is integral to the main result provided in the paper.

Definition 1. Let S be a closed subset of a complete metric space with a metric d defined on it. A *dynamical system* on S is a family of maps $\Gamma(t) : S \to S$, $t \geq 0$ such that

(1) for each $t \geq 0$, $\Gamma(t)$ is continuous from S to S,
(2) for each $u \in S$, $t \to \Gamma(t)u$ is continuous,
(3) for any $u \in S$, $\Gamma(0)u = u$ and
(4) $\Gamma(t_1)\left(\Gamma(t_2)u\right) = \Gamma(t_1 + t_2)u$, for all $t_1, t_2 \geq 0$ and $u \in S$.

Definition 2. For a given $u \in S$, the *trajectory* or the *orbit* of $\Gamma(t)$ for u is

$$\mathscr{B}(u) = \{\Gamma(t)u, t \geq 0\},$$

where u is known as the initial condition.

Definition 3. $v \in S$ is a *steady state* of Γ if

$$\Gamma(t)v = v \qquad \text{for all } t \geq 0.$$

Definition 4. For a given dynamical system, Γ, the steady state, v, is *stable* if for every $\varepsilon > 0$, there exists a $\delta(\varepsilon) > 0$ such that

$$d(u,v) < \delta(\varepsilon)$$

implies

$$d(\Gamma(t)u, \Gamma(t)v) < \varepsilon \text{ for all } u \in S,\ t \geq 0.$$

Definition 5. For a given dynamical system, Γ, the steady state, v, is *asymptotically stable* if it is *stable* and there exists a $\varepsilon > 0$ ball such that $u \in B_\varepsilon$ implies

$$\lim_{t\to\infty} d(\Gamma(t)u, \Gamma(t)v) = 0.$$

where $B_\varepsilon := \{v \in S \,|\, d(u,v) < \varepsilon\}$.

Definition 6. A trajectory $\Gamma(t)u, u \in S$ is *globally asymptotically stable* if it is *stable* and for any initial condition $v \in S$

$$d(\Gamma(t)u, \Gamma(t)v) \to 0 \text{ as } t \to \infty.$$

Definition 7. Given a dynamical system $\Gamma(t), t \geq 0$, a *Lyapunov function* $V : S \to \mathbb{R}$ is a continuous function on S such that

$$\dot{V}(u) = \lim_{t\to 0^+} \sup\{\frac{1}{t}\{V(\Gamma(t)u) - V(u)\} \leq 0$$

for all $u \in S$.

We now state the *Lyapunov stability* theorem.

Theorem 2. Let Γ be a dynamical system defined on S. Let 0 be a steady state in S. Suppose V is a Lyapunov function such that $V(0) = 0$, $\zeta(\|u\|) \geq V(u) \geq \mu(\|u\|)$ and $\dot{V}(u) \leq 0$, $u \in S$, $\|u\| = d(0,u)$ where $\mu(\cdot)$ and $\zeta(\cdot)$ are strictly increasing continuous functions with $\mu(0) = \zeta(0) = 0$ and $\mu(a) > 0$ and $\zeta(a) > 0$ for $a > 0$, then the origin is stable. Additionally suppose $\dot{V}(u) \leq -\gamma(\|u\|)$, where $\gamma(\cdot)$ is continuous strictly increasing with $\gamma(0) = 0$. Then the origin is globally asymptotically stable

3. MAIN RESULT

For a given $\psi_{x,ref}$, the dynamics of $\hat{\psi}_x = \psi_x - \psi_{ref,x}$ are

$$\begin{aligned}\frac{\partial \hat{\psi}_x(x,t)}{\partial t} =& \frac{1}{\mu_0 a^2}\frac{\partial}{\partial x}\left(\frac{\eta_\parallel(x)}{x}\frac{\partial}{\partial x}\left(x\hat{\psi}_x(x,t)\right)\right) \\ &+ R_0 \frac{\partial}{\partial x}\left(\eta_\parallel(x,t) j_{eni}(x,t)\right), \quad (6)\end{aligned}$$

with the boundary conditions

$$\hat{\psi}_x(0,t) = 0 \text{ and } \hat{\psi}_x(1,t) = 0. \qquad (7)$$

where we assume $\eta_\parallel$ is in quasi-steady-state. To simplify notation, when designing the controller, we use ψ instead of $\hat{\psi}$. We propose using a controller of the following form.

$$j_{eni}(x,t) = K_1(x)\psi_x + \frac{d}{dx}(K_2(x)\psi_x), \qquad (8)$$

where $K_1(x)$ and $K_2(x)$ are polynomial gains. We are now ready to state the main theorem of the paper.

Theorem 3. Suppose there exist polynomials $M(x), Z_1(x)$ and $Z_2(x)$ and $\varepsilon > 0$ such that the following holds for $x \in [0,1]$

$$M(x) > \varepsilon I$$

$$\frac{1}{\mu_0 a^2} b_1\left(x, \frac{d}{dx}\right) M(x) + b_2\left(x, \frac{d}{dx}\right) Z_1(x) + b_3\left(x, \frac{d}{dx}\right) Z_2(x) < 0$$

$$\frac{1}{\mu_0 a^2} c_1(x) M(x) + c_2(x) Z_2(x) \leq 0$$

where

$$\begin{aligned} b_1\left((x, \frac{d}{dx}\right) &= f(x)\left(\frac{\eta_{\parallel,x}}{x} - \frac{\eta_\parallel}{x^2}\right) + f'(x)\left(-\frac{\eta_\parallel}{x} + \eta_{\parallel,x}\right) \\ &\quad + f''(x)\eta_\parallel + \frac{f(x)\eta_\parallel}{x}\frac{d}{dx} + \left(f(x)\eta_\parallel + f(x)\eta_{\parallel,x}\right)\frac{d^2}{dx^2} \\ b_2\left(x, \frac{d}{dx}\right) &= -f'(x) + f(x)\frac{d}{dx} \\ b_3\left(x, \frac{d}{dx}\right) &= \eta_{\parallel,x} f'(x) + \eta_\parallel f''(x) + \eta_{\parallel,x} f(x)\frac{d}{dx} + \eta_\parallel f(x)\frac{d^2}{dx^2} \\ c_1(x) &= -\eta_\parallel f(x) \\ c_2(x) &= -2\eta_\parallel f(x) \end{aligned}$$

Note that the spatial dependencies of $\eta_\parallel(x)$ has been dropped from the equations to conserve space. The notation $(\cdot)_x$ and $(\cdot)_{xx}$ represent first order and second order spatial partial derivatives respectively.

Let

$$K_1(x) = R_0^{-1}\eta_\parallel^{-1} Z_1(x) M(x)^{-1}$$

and

$$K_2(x) = R_0^{-1} Z_2(x) M(x)^{-1}.$$

Then the origin of Equation (6) with Controller (8)is globally asymptotically stable.

Proof 3. Let $X = \mathscr{C}(0,1)$ be the set of real valued continuous functions on $(0,1)$. Suppose the hypotheses of the theorem hold. Then $M(x) > \varepsilon, \forall x \in [0,1]$. Then $M(x)^{-1}$ exists and is continuous. Furthermore there exists a $\varepsilon > 0$ such that $M(x)^{-1} > \varepsilon$. Define

$$V(z) = \int_0^1 f(x) M(x)^{-1} z(x)^2 dx. \qquad (9)$$

Where we define $f(x) = x^2(1-x)$. Now, for any $\forall z \in X$,

$$f(x) M(x)^{-1} z(x)^2 \geq \varepsilon x^2 (1-x) z(x)^2, \qquad \text{for all } x \in [0,1].$$

Then $V(z) > 0$ for all $z \neq 0$. We now differentiate V along trajectories of the PDE.

$$\frac{d}{dt} V(\Gamma(t)z) = 2\int_0^1 x^2(1-x) M(x)^{-1} z(x) \left(\frac{d}{dt}\Gamma(t)z\right)(x) dx.$$

where

$$\begin{aligned}\left(\frac{d}{dt}\Gamma(t)z\right)(x) =& \frac{1}{\mu_0 a^2}\frac{\partial}{\partial x}\left(\frac{\eta_\parallel}{x}\frac{\partial}{\partial x}(xz(x))\right) \\ &+ R_0 \frac{\partial}{\partial x}\left(\eta_\parallel K_1(x) z(x) + \eta_\parallel \frac{d}{dx}(K_2(x) z(x))\right)\end{aligned}$$

This yields

$$\begin{aligned}\dot{V}(z) =&2\int_0^1 f(x)M(x)^{-1}\frac{z(x)}{\mu_0 a^2}\frac{\partial}{\partial x}\left(\frac{\eta_\parallel}{x}\frac{d}{dx}\left(xz(x)\right)\right)dx\\ &+2R_0\int_0^1 f(x)M(x)^{-1}z(x)\frac{d}{dx}\left(\eta_\parallel K_1(x)z(x)\right)dx\\ &+2R_0\int_0^1 f(x)M(x)^{-1}z(x)\frac{d}{dx}\left(\eta_\parallel\frac{d}{dx}\left(K_2(x)z(x)\right)\right)dx\end{aligned}$$

Recall $Z_1(x)=\eta_\parallel(x)R_0K_1(x)M(x)$ and $Z_2(x)=R_0K_2(x)M(x)$. Now, we define the function $y(x)=M(x)^{-1}z(x)$. Then $y\in X$ and $z(x)=M(x)y(x)$ and hence we have

$$\begin{aligned}\dot{V}(z) =&2\int_0^1 f(x)\frac{y(x)}{\mu_0 a^2}\frac{d}{dx}\left(\frac{\eta_\parallel}{x}\frac{d}{dx}\left(xM(x)y(x)\right)\right)dx\\ &+2\int_0^1 f(x)y(x)\frac{d}{dx}(Z_1(x)y(x))dx\\ &+2\int_0^1 f(x)y(x)\frac{d}{dx}\left(\eta_\parallel\frac{d}{dx}\left(Z_2(x)y(x)\right)\right)dx\\ &=\frac{2}{\mu_0 a^2}\dot{V}_1(z)+2\dot{V}_2(z)+2\dot{V}_3(z)\end{aligned}$$

where we have split the derivative into three terms. Note we have left the terms in the form $V(z)$ to emphasize that y depends on z. Expanding the first term, we get

$$\begin{aligned}&\dot{V}_1(z)=\int_0^1 f(x)y(x)\frac{d}{dx}\left(\frac{\eta_\parallel}{x}\frac{d}{dx}\left(xM(x)y(x)\right)\right)dx\\ &=-\int_0^1\eta_\parallel\left(\frac{f'(x)}{x}y(x)+\frac{f(x)}{x}y_x(x)\right)\frac{d}{dx}\left(xM(x)y(x)\right)dx\\ &=-\int_0^1\eta_\parallel\left(\frac{f'(x)}{x}y(x)+\frac{f(x)}{x}y_x(x)\right)\Big(M(x)y(x)\\ &\qquad\qquad+xM_x(x)y(x)+xM(x)y_x(x)\Big)dx\\ &=-\int_0^1\eta_\parallel\left(\frac{f'(x)M(x)}{x}+f'(x)M_x(x)\right)y(x)^2dx\\ &-\int_0^1\eta_\parallel\left(f(x)M(x)\right)y_x(x)^2dx\\ &-\int_0^1\eta_\parallel\left(f'(x)M(x)+\frac{f(x)M(x)}{x}+f(x)M_x(x)\right)y(x)y_x(x)dx\\ &=-\int_0^1\eta_\parallel\left(\frac{f'(x)M(x)}{x}+f'(x)M_x(x)\right)y(x)^2dx\\ &-\int_0^1\eta_\parallel\left(f(x)M(x)\right)y_x(x)^2dx\\ &+\tfrac{1}{2}\int_0^1\eta_\parallel\Big(f''(x)M(x)+f'(x)M_x(x)+\frac{xf'(x)-f(x)}{x^2}M(x)\\ &+\frac{f(x)}{x}M_x(x)+f'(x)M_x(x)+f(x)M_{xx}(x)\Big)y(x)^2dx\\ &+\tfrac{1}{2}\int_0^1\eta_{\parallel,x}\left(f'(x)M(x)+\frac{f(x)M(x)}{x}+f(x)M_x(x)\right)y(x)^2dx\\ &=\tfrac{1}{2}\int_0^1 y(x)^2b_1\left(x,\frac{d}{dx}\right)M(x)dx+\tfrac{1}{2}\int_0^1 y_x(x)^2c_1(x)M(x)dx.\end{aligned}$$

where we have used that $\lim_{x\to 0}f(x)/x=\lim_{x\to 0}f'(x)/x=0$ and $y(1)=0$.

Performing integration by parts on the second term, we have

$$\begin{aligned}\dot{V}_2(z)&=\int_0^1 f(x)Z_{1,x}(x)y(x)^2dx+\int_0^1 f(x)Z_1(x)y(x)y_x(x)dx\\ &=\int_0^1\left(f(x)Z_{1,x}(x)-\tfrac{1}{2}f'(x)Z_1(x)-\tfrac{1}{2}f(x)Z_{1,x}(x)\right)y(x)^2dx\\ &=\int_0^1\left(\tfrac{1}{2}f(x)\frac{d}{dx}-\tfrac{1}{2}f'(x)\right)Z_1(x)y(x)^2dx\\ &=\tfrac{1}{2}\int_0^1 y(x)^2b_2\left(x,\frac{d}{dx}\right)Z_1(x)dx\end{aligned}$$

where we have used that $y(0)=y(1)=0$.

Performing integration by parts on the third term, we have

$$\begin{aligned}&\dot{V}_3(z)=\int_0^1 f(x)y(x)\frac{d}{dx}\left(\eta_\parallel\frac{d}{dx}\left(Z_2(x)y(x)\right)\right)dx\\ &=-\int_0^1\eta_\parallel y(x)\left(f'(x)y(x)\right)\left(Z_{2,x}(x)y(x)+Z_2(x)y_x(x)\right)dx\\ &-\int_0^1\eta_\parallel y(x)\left(f(x)y_x(x)\right)\left(Z_{2,x}(x)y(x)+Z_2(x)y_x(x)\right)dx\\ &=-\int_0^1\eta_\parallel\left(f'(x)Z_{2,x}(x)y(x)\right)y(x)^2+\eta_\parallel\left(f(x)Z_2(x)\right)y_x(x)^2dx\\ &-\int_0^1\eta_\parallel\left(f'(x)Z_2(x)+f(x)Z_{2,x}(x)\right)y(x)y_x(x)dx\\ &=-\int_0^1\eta_\parallel\left(f'(x)Z_{2,x}(x)\right)y(x)^2+\eta_\parallel\left(f(x)Z_2(x)\right)y_x(x)^2dx\\ &+\tfrac{1}{2}\int_0^1\eta_\parallel\left(f''(x)Z_2(x)+2f'(x)Z_{2,x}(x)+f(x)Z_{2,xx}(x)\right)y(x)^2dx\\ &+\tfrac{1}{2}\int_0^1\eta_{\parallel,x}\left(f'(x)Z_2(x)+f(x)Z_{2,x}(x)\right)y(x)^2dx\\ &=-\int_0^1\eta_\parallel\left(f(x)Z_2(x)\right)y_x(x)^2dx\\ &+\tfrac{1}{2}\int_0^1\eta_\parallel\left(f''(x)Z_2(x)+f(x)Z_{2,xx}(x)\right)y(x)^2dx\\ &+\tfrac{1}{2}\int_0^1\eta_{\parallel,x}\left(f'(x)Z_2(x)+f(x)Z_{2,x}(x)\right)y(x)^2dx\\ &=\tfrac{1}{2}\int_0^1 y(x)^2b_3\left(x,\frac{d}{dx}\right)Z_2(x)dx+\tfrac{1}{2}\int_0^1 y_x(x)^2c_2(x)Z_2(x)dx\end{aligned}$$

where we have used that fact that $y(0)=0$ and $y(1)=0$. Combining the three terms, we obtain

$$\begin{aligned}\dot{V}(z)=&\int_0^1 y_x(x)^2\left(\frac{1}{\mu_0 a^2}c_1M(x)+c_2Z_2(x)\right)dx\\ &+\tfrac{1}{2}\int_0^1 y(x)^2\left(\frac{1}{\mu_0 a^2}b_1M(x)+b_2Z_1(x)+b_3Z_2(x)\right)dx\end{aligned}$$

where we have suppressed the dependencies of b_i and c_i for clarity. Because $M(x)>0$ for $x\in[0,1]$, is $z\neq 0$, then $y\neq 0$. Hence we conclude that if the conditions of the theorem are satisfied then $\dot{V}(z)<0$ for $z\neq 0$. Thus we conclude asymptotic stability of the system described by (6) with the controller (8).

The conditions of the theorem may be tested using sum-of-squares optimization. This is done in the following sections. The theorem uses a notion of duality and full-state feedback synthesis which was introduced in Peet and Papachristodoulou [2009]. Note that there are several limitations of this main result. In particular, it gives no bound on the current voltage of the controller, nor does it attempt to constrain the controller to a gaussian shape. The bound on the controller can be implemented using a constraint of the form

$$K_1(x)\psi_{x,ref}(x) = R_0^{-1}\eta_{\|}^{-1}Z_1(x)M(x)^{-1}\psi_{x,ref}(x) \leq 10^7 A$$

for some error reference profile, $\psi_{x,ref}$. This will lead to a functional constraint of the form

$$Z_1(x) \leq R_0\,\eta_{\|}(x)M(x) * 10^7 A,$$

which can be included via SOSTOOLS.

4. DISCRETIZATION OF THE SYSTEM MODEL

Once we have designed a controller satisfying Theorem 3 using SOSTOOLS, we would like to simulate the dynamics under realistic operating conditions in order to verify convergence. To do this we discretize the controlled model in space to get a system of coupled ODEs. The system of ODEs can then be solved using ODE solvers in MATLAB.

Since we have Dirichlet boundary conditions

$$\psi_x(0,t) = a \text{ and } \psi_x(1,t) = b,$$

we will be discretizing the interior of the spatial domain, which in this case is $(0,1)$. Spatial domain is discretized with N uniformly-spaced interior points with distance Δx between them. The first and the N^{th} point are located at the distance $\Delta x/2$ from the left and right boundary of the domain, respectively. Then the grid size, Δx, is calculated as $\Delta x = 1/N$. The discrete variables of the function $u(x,t)$ are calculated at $x_j = (j-1/2)\Delta x$ for $j = 1,\cdots,N$.

Expanding (6) with the controller (8) one can easily observe that we will obtain an equation of the form

$$\dot{\psi}_x(x,t) = \underbrace{\alpha(x)\psi_x}_{1} + \underbrace{\beta(x)\frac{\partial\psi_x}{\partial x}}_{2} + \underbrace{\gamma(x)\frac{\partial^2\psi_x}{\partial x^2}}_{3}, \tag{10}$$

where $\alpha(x)$, $\beta(x)$ and $\gamma(x)$ are the relevant coefficients.

We will now describe the scheme used for the discretization of Eq. (10). We denote the values of the functions $\psi_x(x,t), \alpha(x), \beta(x)$ and $\gamma(x)$ at the grid points x_j as $\psi_{x,j}(t), \alpha_j, \beta_j$ and γ_j, respectively. Then the spatial discretization of the first term is simply

$$L[\alpha(x)\,\psi_x] = \alpha_j\psi_{x,j}(t), \tag{11}$$

for the second term we use upwind-differentiation scheme in order to ensure stability:

$$L[\beta(x)\frac{\partial\psi_x}{\partial x}] = \begin{cases} \dfrac{\beta_j}{\Delta x}\left(\psi_{x,j}(t) - \psi_{x,j-1}(t)\right) & \text{if } \beta_j < 0 \\ \\ \dfrac{\beta_j}{\Delta x}\left(\psi_{x,j+1}(t) - \psi_{x,j}(t)\right) & \text{if } \beta_j \geq 0 \end{cases}, \tag{12}$$

and the third term is discretized with the second-order central difference scheme

$$L[\gamma(x)\frac{\partial^2\psi_x}{\partial x^2}] = \frac{\gamma_j}{\Delta x^2}\left(\psi_{x,j+1}(t) - 2\psi_{x,j}(t) + \psi_{x,j-1}(t)\right). \tag{13}$$

With the help of Eqs. (11)–(13), the spatial discretization of Eq. (10) becomes

$$L[\dot{\psi}_{x,j}(t)] = [\,e_{j1}\;\; e_{j2}\;\; e_{j3}\,]\begin{bmatrix}\psi_{x,j-1}(t)\\ \psi_{x,j}(t)\\ \psi_{x,j+1}(t)\end{bmatrix}, \tag{14}$$

where

$$\begin{aligned} e_{j1} &= -\frac{\beta_j}{\Delta x} + \frac{\gamma_j}{\Delta x^2}, \\ e_{j2} &= \alpha_j + \frac{\beta_j}{\Delta x} - 2\frac{\gamma_j}{\Delta x^2}, \\ e_{j3} &= \frac{\gamma_j}{\Delta x^2}, \end{aligned} \tag{15}$$

if $\beta_j < 0$, and

$$\begin{aligned} e_{j1} &= \frac{\gamma_j}{\Delta x^2}, \\ e_{j2} &= \alpha_j - \frac{\beta_j}{\Delta x} - 2\frac{\gamma_j}{\Delta x^2}, \\ e_{j3} &= \frac{\beta_j}{\Delta x} + \frac{\gamma_j}{\Delta x^2}, \end{aligned} \tag{16}$$

if $\beta_j \geq 0$.

Boundary conditions: Note that Eqs. (12)–(16) are only valid for the points $j = 2\ldots N-1$, and not for $j = 1$ and $j = N$, since, first, equations at $j = 1$ and $j = N$ require the values at the the domain boundaries $\psi_{x,0}(t)$ and $\psi_{x,N+1}(t)$ and, second, the discretization stencil must be changed to accommodate the fact that $j = 1$ and $j = N$ are spaced only $\Delta x/2$ from the boundaries, and not Δx. The boundary values are available from the Dirichlet boundary conditions $\psi_{x,0}(t) = a$ and $\psi_{x,N+1}(t) = b$. Spatial discretization of the second term at the point $j = 1$ given by Eq. (12) will be modified as

$$L[\beta(x)\frac{\partial\psi_x}{\partial x}] = \begin{cases} \dfrac{\beta_1}{\Delta x/2}\left(\psi_{x,1}(t) - \psi_{x,0}(t)\right) & \text{if } \beta_1 < 0 \\ \\ \dfrac{\beta_1}{\Delta x}\left(\psi_{x,2}(t) - \psi_{x,1}(t)\right) & \text{if } \beta_1 \geq 0 \end{cases} \tag{17}$$

and similarly for $j = N$. Spatial discretization of the third term at the point $j = 1$ given by Eq. (13) is

$$L[\gamma(x)\frac{\partial^2\psi_x}{\partial x^2}] = \frac{\gamma_j}{\Delta x/2 + \Delta x/4}\left(\psi'_{x,3/2}(t) - \psi'_{x,1/2}(t)\right) = \frac{\gamma_j}{\Delta x/2 + \Delta x/4}\left(\frac{\psi_{x,1}(t) - \psi_{x,0}(t)}{\Delta x/2} + \frac{\psi_{x,2}(t) - \psi_{x,1}(t)}{\Delta x}\right), \tag{18}$$

where $\psi'_{x,1/2}$ and $\psi'_{x,3/2}$ denote spatial derivative of ψ_x at the midpoints of the intervals $[x_0,x_1]$ and $[x_1,x_2]$, respectively. Similar discretizaton can be constructed for $j = N$.

5. SIMULATION

For the purpose of simulation, the following values are taken from the data of the *tore supra* tokamak as

$$I_p(t) = 0.6MA \text{ and } B_{\phi_0} = 1.9T,$$

where $I_p(t)$ is the plasma current and B_{ϕ_0} is the toroidal magnetic field at the plasma center.

Given a q-profile, the corresponding ψ_x-profile, for $x \in (0,1)$, can be computed using (1), where $a = .72m$ for the *tore supra* tokamak. The boundary values for ψ_x are calculated using the magnetic center location for the *tore supra* tokamak, which is, $R_0 = 2.38m$ and the equations (3) and (4) to get

$$\psi_x(0,t) = 0 \text{ and } \psi_x(1,t) = -0.2851. \tag{19}$$

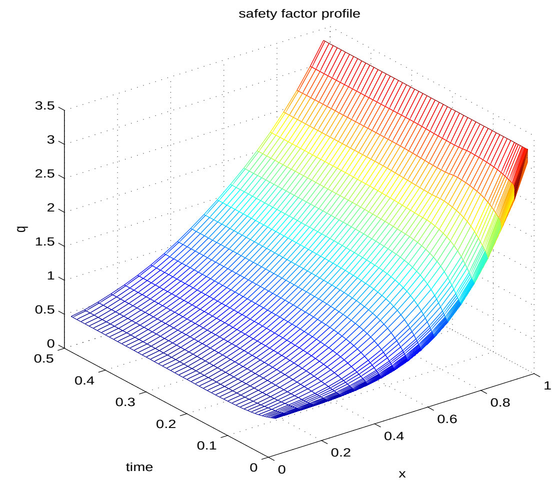

Fig. 1. Time evolution of the safety factor profile or the q-profile. For most tokamaks, the q-profile attains it's minimum near the plasma center, $x = 0$ and increases outwards.

Suppose we want to stabilize a reference safety factor profile, q_{ref} given the initial profile, q_{init}. We would then stabilize the reference profile $\psi_{x,ref}$ obtained from q_{ref}, provided with an initial ψ_x-profile, $\psi_{x,init}$, obtained from q_{init},

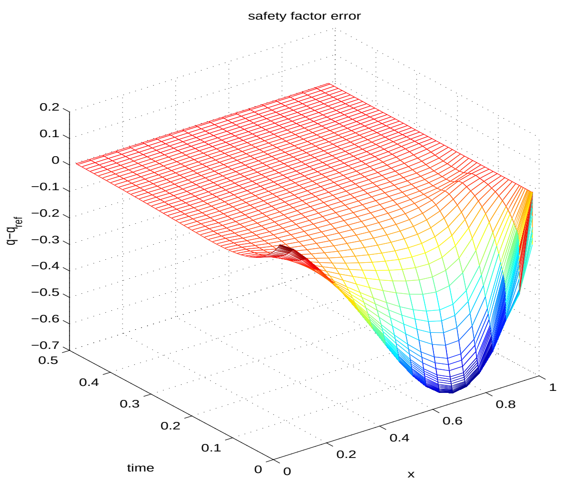

Fig. 2. Time evolution of the q-profile Error, $q(x,t) - q_{ref}(x,t)$. Here x is the normalized spatial variable.

Finally, we include real-time plasma resistivity measurements from the *tore supra* tokamak for shot TS 35109 in the simulation. The attached figures show the time evolution of the q-profile until $t = .5s$. Fig. 1 presents the time evolution of $q(x,t)$ and Fig. 2 presents the evolution of the error, $\hat{q} = q - q_{ref}$. Fig. 3 and Fig. 4 present the corresponding ψ_x and $\hat{\psi}_x = \psi_x - \psi_{x,ref}$ profiles respectively.Fig. 5 shows the control effort

$$j_{eni}(x,t) = K_1(x)\psi_x + \frac{d}{dx}(K_2(x)\psi_x).$$

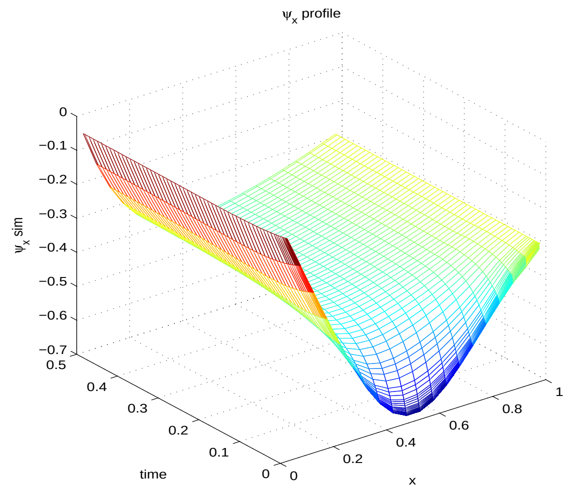

Fig. 3. Time evolution of ψ_x-profile corresponding to the q-profile in Fig. 1

.

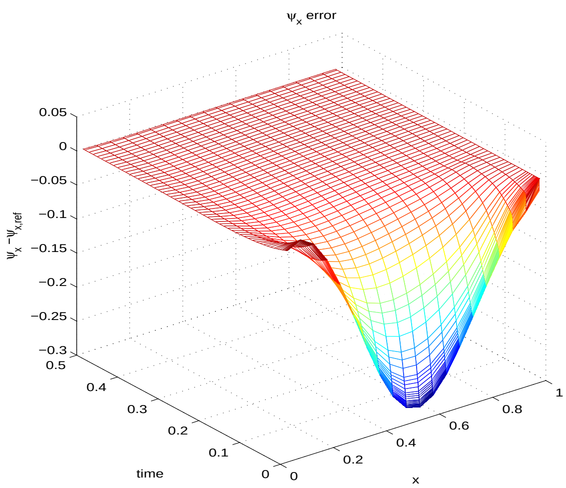

Fig. 4. ψ_x-profile error, $\psi_x - \psi_{x,ref}$. Here $\psi_{x,ref}$ is obtained from the reference q-profile, q_{ref}.

6. CONCLUSIONS

In this paper we present a methodology to synthesize full-state feedback controllers for the stabilization of the safety factor profile using *sum-of-squares* polynomials. This methodology is based on a dual version of the Lyapunov inequality. The methods presented here can also be applied to other systems described by PDEs. There are numerous directions for future work including consideration of more realistic models, more general forms of controller and more sophisticated Lyapunov functions.

7. ACKNOWLEDGEMENTS

We would like to thank Dr. Yulia Peet of Argonne National Laboratory for work on numerical solution of the partial differential equations and other contributions to the paper.

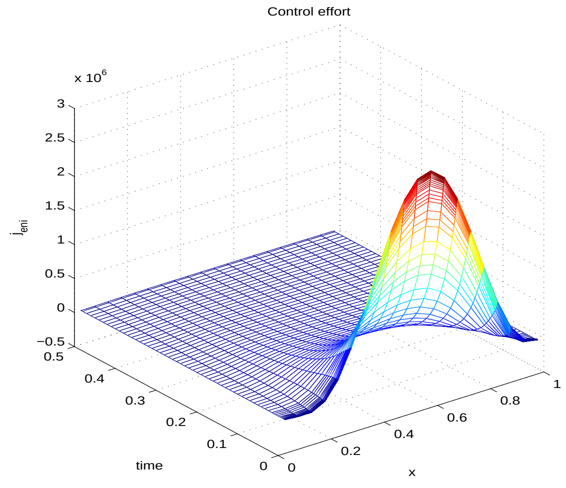

Fig. 5. External non-inductive current deposit, $j_{eni}(x,t)$. The actuators for the control input are the Radio Frequency(RF) antennas. An example would be the Lower Hybrid Current Drive(LHCD) antenna.

REFERENCES

M. Ariola and A. Pironti. *Magnetic Control of Tokamak Plasmas*. Springer Verlag, 2008.

J. Blum. *Numerical simulation and optimal control in plasma physics*. John Wiley &. Sons, 1988.

L. Blum. *Complexity and real computation*. Springer Verlag, 1998.

C.J. Campbell and J.H. Laherrère. The end of cheap oil. *Scientific American*, 278(3):60–5, 1998.

JW Connor, RJ Hastie, HR Wilson, and RL Miller. Magnetohydrodynamic stability of tokamak edge plasmas. *Physics of Plasmas*, 5:2687, 1998.

R.F. Curtain and H.J. Zwart. *An introduction to infinite-dimensional linear systems theory*. Springer, 1995.

L.G. Eriksson, C. Fourment, V. Fuchs, X. Litaudon, CD Challis, F. Crisanti, B. Esposito, X. Garbet, C. Giroud, N. Hawkes, et al. Discharges in the JET tokamak where the safety factor profile is identified as the critical factor for triggering internal transport barriers. *Physical review letters*, 88(14):145001, 2002.

MA Firestone. Analysis of modern optimal control theory applied to plasma position and current control in TFTR. *Plasma Science, IEEE Transactions on*, 10(2):105–115, 2007.

X. Garbet, Y. Baranov, G. Bateman, S. Benkadda, P. Beyer, R. Budny, F. Crisanti, B. Esposito, C. Figarella, C. Fourment, et al. Micro-stability and transport modelling of internal transport barriers on JET. *Nuclear Fusion*, 43:975, 2003.

A.M. Lyapunov. The general problem of the stability of motion. *International Journal of Control*, 55(3):531–534, 1992.

D. Moreau, D. Mazon, M. Ariola, G.D. Tommasi, L. Laborde, F. Piccolo, F. Sartori, T. Tala, L. Zabeo, A. Boboc, et al. A two-time-scale dynamic-model approach for magnetic and kinetic profile control in advanced tokamak scenarios on JET. *Nuclear Fusion*, 48:106001, 2008.

Y. Nesterov and A. Nemirovsky. Interior point polynomial methods in convex programming. *Studies in applied mathematics*, 13, 1994.

A. Papachristodoulou and M.M. Peet. On the analysis of systems described by classes of partial differential equations. In *Decision and Control, 2006 45th IEEE Conference on*, pages 747–752. IEEE, 2007.

M. Peet, A. Papachristodoulou, and S. Lall. Positive forms and stability of linear time-delay systems. In *Decision and Control, 2006 45th IEEE Conference on*, pages 187–193. IEEE, 2007.

M. M. Peet and A. Papachristodoulou. Inverses of positive linear operators and state feedback design for time-delay systems. In *8th IFAC Workshop on Time-Delay Systems*, 2009.

A. Pironti and M. Walker. Control of tokamak plasmas: introduction to a special section. *Control Systems Magazine, IEEE*, 25(5):24–29, 2005.

S. Prajna, A. Papachristodoulou, and P.A. Parrilo. Introducing SOSTOOLS: A general purpose sum of squares programming solver. In *IEEE conference on decision and control*, volume 1, pages 741–746. Citeseer, 2001.

TJJ Tala, JA Heikkinen, VV Parail, Y.F. Baranov, and SJ Karttunen. ITB formation in terms of ωE$\times$ B flow shear and magnetic shear s on JET. *Plasma Physics and Controlled Fusion*, 43:507, 2001.

J. Wesson and DJ Campbell. *Tokamaks*. Oxford University Press, USA, 2004.

E. Witrant, E. Joffrin, S. Brémond, G. Giruzzi, D. Mazon, O. Barana, and P. Moreau. A control-oriented model of the current profile in tokamak plasma. *Plasma Physics and Controlled Fusion*, 49:1075, 2007.